

MACA Algorithm to Accelerate Modeling of Eddy Current Position Sensor

Yang Bao¹, Zhiwei Liu², and Jiming Song¹

¹Department of Electrical and Computer Engineering
Iowa State University, Ames, IA 50011, USA
brianbao@iastate.edu, jisong@iastate.edu

²Department of Information Engineering
East China Jiaotong University, Nanchang, Jiangxi 330013, China
zwliu1982@hotmail.com

Abstract — In this paper, we proposed a Modified Adaptive Cross Approximation (MACA) algorithm method to model an eddy current probe used as position sensor in Nondestructive Evaluation (NDE). Eddy current based position sensor can be used when optical aids cannot to guide the position of the coil. We use surface integral equation technique with selected Stratton-Chu formulation and apply MACA algorithm to accelerate the calculation of impedance change for the position sensor. Good performance of proposed method is demonstrated with numerical examples.

Index Terms — Eddy current nondestructive evaluation, modified adaptive cross approximation, position sensor.

I. INTRODUCTION

Eddy current technique is a high-speed nondestructive method to detect corrosion, cracks or flaws in metallic tubes. Thousands of tubes are used in heat exchangers and steam generators to increase the amount of heat transferred. Eddy current technique is especially important in nuclear power plants where reused, contaminated water must be prevented from mixing with fresh water that will be returned to the environment [1]. To minimize the risk of leakage from the tubes becomes the aim of eddy current technique. For the heat exchangers, in the presence of coolant, the coil position cannot be guided by optical aid, while eddy current technique can be used to sense it [2].

Finite element method has been applied for the modeling of eddy current nondestructive evaluation (NDE) problems for the tubes [3-4], but the drawback is that it needs to discretize the whole solution domain which results in consuming too much computational resource. Adaptive cross approximation (ACA) was proposed by Bebendorf [5], with the help of tree structure, it replaces the well separated far-block interactions by low rank approximation and compute the elements from diagonal and near block interactions with

full matrix. Purely algebraic and kernel independent are the key features for ACA algorithm. ACA algorithm uses only part of the elements from the original matrix and makes every skeletons a kind of cross over all the other pivot rows and columns. In this paper, we proposed the modified ACA (MACA) to accelerate boundary element method (BEM) for 3D eddy current modeling of the tubes. MACA is based on the rule that when the diagonal interactions are dominant compared with the far block interactions, these far block interactions can be neglected to decrease the memory requirement and CPU time.

II. MACA BASED BEM

The details of ACA algorithm are shown in [5-7], the details of the selected Stratton-Chu formulation based BEM are shown in [8] and ACA based BEM is shown in [9]. The discretized form of BEM matrix has seven nonzero matrices with four kinds of dimensions (number of edges by number of edges, number of patches by number of edges, number of edges by number of patches and number of patches by number of patches), as:

$$\begin{bmatrix} 0.5\mathbf{T} - \mathbf{K}_1^\times & 0 & \mathbf{R}_1^\times \\ -i\mu_2/\mu_1 \mathbf{L}_2^\times & 0.5\mathbf{T} + \mathbf{K}_2^\times & 0 \\ \mu_2/\mu_1 \mathbf{K}_2^n & ik_2^2 \mathbf{L}_2^n & 0.5\mathbf{D} - \mathbf{R}_2^n \end{bmatrix}, \quad (1)$$

where k is the wavenumber, μ is permeability, subscript $i = 1, 2$ stand for medium 1 (air) or medium 2 (metal), the superscript \times and n denote the cross or dot products with normal unit vector $\hat{\mathbf{n}}$, and give the tangential and normal components, respectively. \mathbf{R} , \mathbf{L} , \mathbf{K} , \mathbf{T} , \mathbf{D} are shown in [8], \mathbf{D} is a diagonal matrix, \mathbf{T} is a diagonal-dominant sparse matrix, \mathbf{L} is the electric (magnetic) field due to the electric (magnetic) current directly, \mathbf{K} is the electric (magnetic) field due to the magnetic (electric) current, and \mathbf{R} is the electric (magnetic) field due to the electric (magnetic) charge. The dimensions of each matrix are due to number of basis and testing functions.

Octal tree structure is used to divide the object into

blocks which will leads to diagonal, near and far block interactions. For the diagonal and near block interactions, full matrices will be saved, while for the far block interactions, MACA is applied to approximate it which leads to the reduction of the memory requirement.

The basic idea for MACA is that due to the nature of Green's function: localized static field in medium 1 and exponential decay in medium 2, the bigger distance between two far blocks, the smaller interaction between them. In the impedance matrix, when the diagonal block interaction is much larger than the far block interactions, we can neglect these far block interactions which has almost no effects to the accuracy but with a reduction to the total memory requirement. We define the threshold value by:

$$\Delta_1 = |Z_{mn}|/|Z_{11}|, \quad (2)$$

where Z_{mn} is the interaction between far block pair box m and box n , Z_{11} stands for the first box's self-interaction. By controlling the threshold value, we can decide how to ignore the small far block interactions.

We use a curve strip as an example to show the way MACA works. In Fig. 1, four periods of curve strips are shown. The radius of one period is 1.5 mm, height is 4 mm. We can regard one period as one nonempty box with 32 edges and patches. Expand these four periods vertically to get 60 periods. Totally there are 60 nonempty boxes with 1920 edges and patches.

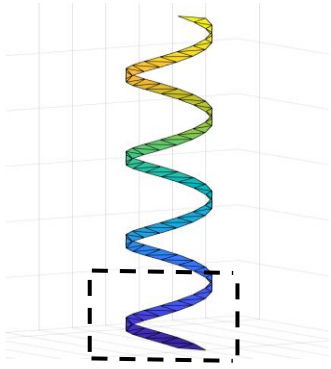


Fig. 1. Four periods of curve strip. One period of curve strip is circled with dash lines.

Then we compare box 1's self-interaction with the interaction between box 1 and other far blocks. Since we have seven nonempty matrices, we need to apply MACA to test all of them. We define other two relative differences as:

$$\Delta_2 = |\Delta Z_{mn}|/|Z_{mn}|, \quad (3)$$

$$\Delta_3 = |\Delta Z_{mn}|/|Z_{11}| = \Delta_1 \Delta_2, \quad (4)$$

where $|\Delta Z_{mn}|$ is the difference between original matrix and approximated matrix with ACA algorithm. For all the tests, we set the threshold value $\Delta_1 = 10^{-4}$ which means that we can neglect the far block interactions

when they are 10^4 times smaller than diagonal ones.

Let's take the submatrix $\mu_2/\mu_1 \mathbf{K}_2^n$ which is the normal component of the magnetic field due to the electric current in region 2 with dimension of number of patches by number of edges as an example. Three kinds of relative differences for the interaction between box 1 and its far block interactions are plotted in Fig. 2.

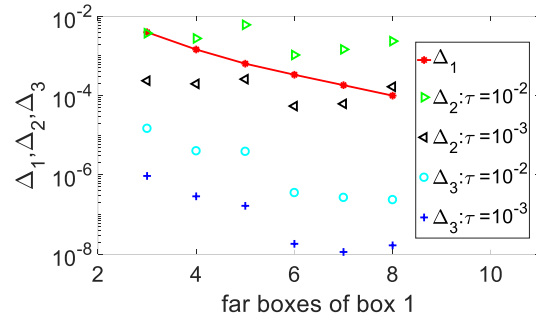


Fig. 2. Relative differences between box 1 and its far block interactions. The relative differences are defined in (2)-(4) for the submatrix $\mu_2/\mu_1 \mathbf{K}_2^n$ which is the normal component of the magnetic field due to the electric current in region 2.

The box 1's far blocks start from box 3. We can see from Fig. 2 that with the increase in accuracy of ACA, more accurate Δ_2 , Δ_3 are observed. When ACA tolerance τ is 10^{-2} , from Δ_3 , $|\Delta Z_{mn}|$ is 10^5 times smaller than $|Z_{11}|$ which means the difference between original interaction and the approximated one by ACA is very small compared to the diagonal block interaction. As the distance increases, Δ_1 decreases due to the nature of Green's function. After the interaction between box 1 and box 7, Δ_1 will be smaller than 10^{-4} which stands for that the far block interaction is small enough compared to diagonal one. We can neglect the box 1's far block interactions from box 8 to box 60.

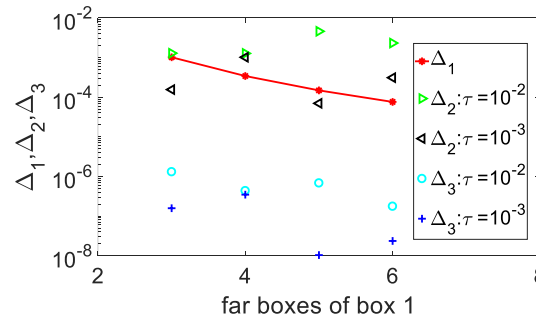


Fig. 3. Relative differences between box 1 and its far block interactions. The relative differences are defined in (2)-(4) for the submatrix $0.5\mathbf{D} - \mathbf{R}_2^n$ which is the normal component of the magnetic field due to the magnetic charge in region 2.

Figure 3 shows the relative differences for the submatrix $0.5\mathbf{D} - \mathbf{R}_2^n$ which is the normal component of the magnetic field due to the magnetic charge in region 2 with the dimension of number of patches to number of patches. From Fig. 3, conclusions can be drew that with the threshold value 10^{-4} , we can neglect the box 1's far block interactions from box 6 to box 60.

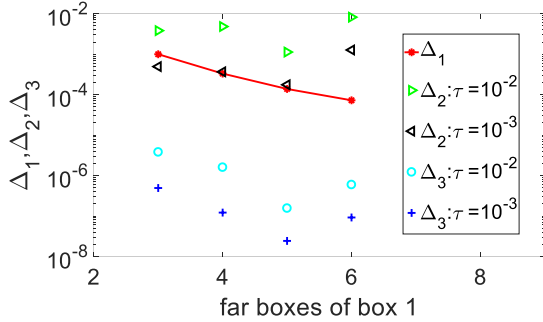


Fig. 4. Relative differences between box 1 and its far block interactions. The relative differences are defined in (2)-(4) for the submatrix $0.5\mathbf{T} + \mathbf{K}_2^x$ which is the tangential component of the electric field due to the magnetic current in region 2.

Figure 4 shows the relative differences for the submatrix $0.5\mathbf{T} + \mathbf{K}_2^x$ which is the tangential component of the electric field due to the magnetic current in region 2 with the dimension of number of edges to number of edges. From Fig. 4, with the threshold value 10^{-4} , we can neglect the box 1's far block interactions from box 6 to box 60.

We do the same test to other submatrices. Figure 5 shows Δ_1 for all the seven submatrices as a summary. It is observed that in the semi-logarithm plot, curves for five submatrices associated with medium 2 are straight lines because the Green function decreases exponentially in the metal. The curves for two submatrices for medium 1 decrease as $1/r^2$ which is due to the static behavior for the Green function in the air region. The three submatrices $0.5\mathbf{T} - \mathbf{K}_1^x$, $0.5\mathbf{T} + \mathbf{K}_2^x$, $0.5\mathbf{D} - \mathbf{R}_2^n$ are diagonal dominant and give much smaller Δ_1 than that of other submatrices for non-diagonal block interactions.

Also, for all the seven submatrices, with the threshold value 10^{-4} , we can neglect a lot of far block interactions which are much smaller than the diagonal ones. For the submatrix $0.5\mathbf{T} - \mathbf{K}_1^x$, $-i\mu_2/\mu_1\mathbf{L}_2^x$, \mathbf{R}_1^x , we can neglect the box 1's far block interactions from box 8, box 14, box 16 to box 60, separately. Above all, we can save a lot of memory while keeping almost same

accuracy because the interactions neglected are trivial.

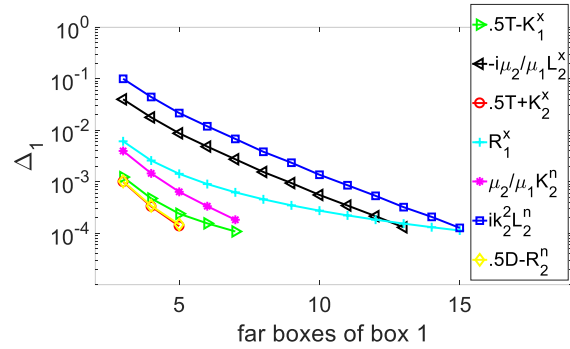


Fig. 5. Relative difference between box 1's self interaction and its far block interactions for seven nonempty submatrices.

III. PERFORMANCE OF MACA

This section shows the performance of MACA when it applies to the steam generator tubes in power plants. The eddy current testing was applied to evaluate the condition of metallic parts in a sodium cooled fast reactor. Coil has the same axis as that of the tube. The coil and tube's parameters are in [10]. All the calculations are done in double precision.

The frequency is 50 kHz, the truncation height is 20 times of skin depth. The impedance change calculated agrees well with that in [10] as shown in Table 1.

Table of impedance change (mΩ) due to tube

Tao & Bowler [10]	8.873 + 21.95i
BEM	8.862 + 21.96i
ACA	8.862 + 21.96i
MACA	8.867 + 21.96i

From Table 1, a good accuracy can be observed in both the real and imaginary parts of impedance changes calculated by semi-analytical method, BEM, ACA and MACA. MACA gets a very good agreement with ACA, semi-analytical method and BEM that the relative differences for real and imaginary parts of impedance changes are smaller than 1%.

For the complexity, the frequency is 30 kHz, with the fixed height of the tube, increase the number of unknowns by decreasing the mesh sizes. The number of unknowns is approximately from 10,000 to 50,000. ACA tolerance is $\tau = 10^{-3}$ and threshold value Δ_1 for MACA is 10^{-4} which results in the relative difference for the impedance changes between BEM and ACA or MACA smaller than 1%. The complexity for memory requirement and CPU time are shown in Figs. 6 (a) and (b).

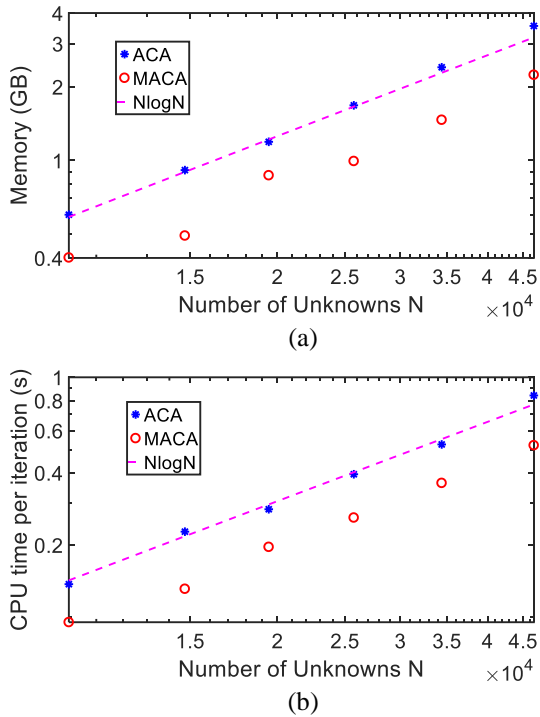


Fig. 6. Performance of ACA and MACA based BEM method for the coil inside the tube. With fixed geometry, different mesh sizes, and number of unknowns from 10,000 to 50,000 at 30 kHz. (a) Memory requirement and (b) CPU time.

From Fig. 6, the complexity of ACA is $O(N \log N)$ for both memory requirement and CPU time per iteration which agrees well with [6]. MACA has more memory and CPU time saving comparing with that of ACA. MACA is very suitable for the tube shape problems because it can neglect the smaller far block interactions which can efficiently deal with the required large truncated area of BEM.

IV. CONCLUSION

The MACA based BEM has proposed to accelerate the modeling of tubes for eddy current NDE problems. With the help of MACA, more memory saving are observed comparing with the ACA algorithm. Performance are shown to validate our proposed method.

ACKNOWLEDGMENT

This work is supported in part by the IU Program of the Center for Nondestructive Evaluation at Iowa State University, by China Scholarship Council, by National Natural Science Foundation of China (61601185) and by Natural Science Foundation of Jiangxi Province (20171ACB21040).

REFERENCES

- [1] NDT resource center, "Tube inspection," [Online]. Available at: <https://www.nde-ed.org/EducationResources/CommunityCollege/EddyCurrents/Applications/tubeinspection.htm>. [Accessed: 19 Apr., 2018].
- [2] T. Wu and J. R. Bowler, "Electromagnetic modeling of an eddy-current position sensor for use in a fast reactor," in *43rd Annual Review of Progress in Quantitative Nondestructive Evaluation*, vol. 1806, Atlanta, GA, USA, July 2016.
- [3] N. Ida and W. Lord, "A finite element model for three dimensional eddy current NDT phenomena," *IEEE Trans. on Magnetics*, vol. 21, no. 6, pp. 2635-2643, Nov. 1985.
- [4] S. J. Song and Y. K. Shin, "Eddy current flaw characterization in tubes by neural networks and finite element modeling," *NDT & E International*, vol. 33, no. 4, pp. 233-243, June 2000.
- [5] M. Bebendorf, "Approximation of boundary element matrices," *Numer. Math.*, vol. 86, no. 4, pp. 565-589, June 2000.
- [6] K. Zhao, M. N. Vouvakis, and J. F. Lee, "The adaptive cross approximation algorithm for accelerated method of moments computations of EMC," *IEEE Trans. Electromagn. Compat.*, vol. 47, no. 4, pp. 763-773, Nov. 2005.
- [7] S. Börm and L. Grasedyck, "Hybrid cross approximation of integral operators," *Numer. Math.*, vol. 101, no. 2, pp. 221-249, Aug. 2005.
- [8] M. Yang, "Efficient Method for Solving Boundary Integral Equation in Diffusive Scalar Problem and Eddy Current Nondestructive Evaluation," *Ph.D. dissertation*, Iowa State Uni., Ames, IA, USA, 2010.
- [9] Y. Bao, Z. W. Liu, and J. M. Song, "Adaptive cross approximation algorithm for accelerating BEM in eddy current nondestructive evaluation," *Journal of Nondestructive Evaluation*, under review.
- [10] T. Wu and J. R. Bowler, "Eddy-current induction by a coil whose axis is perpendicular to that of a tube," *IEEE Trans. Magnetics*, vol. 53, no. 7, pp. 1-9, July 2017.